Geophysical Research Letters

RESEARCH LETTER
10.1029/2022GL102640

Enhanced Continental Weathering as a Trigger for the End-Devonian Hangenberg Crisis

Wenkun Qie[1], Junpeng Zhang[1], Genming Luo[2], Thomas J. Algeo[2,3,4], Bo Chen[1], Lei Xiang[1], Kun Liang[1], Xianyi Liu[5], Philip A. E. Pogge von Strandmann[5,6], Jitao Chen[1], and Xiangdong Wang[7]

[1]State Key Laboratory of Palaeobiology and Stratigraphy, Nanjing Institute of Geology and Palaeontology, Chinese Academy of Sciences, Nanjing, China, [2]State Key Laboratory of Biogeology and Environmental Geology, School of Earth Sciences, China University of Geosciences, Wuhan, China, [3]State Key Laboratory of Geological Processes and Mineral Resources, China University of Geosciences, Wuhan, China, [4]Department of Geosciences, University of Cincinnati, Cincinnati, OH, USA, [5]LOGIC, Department of Earth Sciences, University College London, London, UK, [6]MIGHTY, Institute of Geosciences, Johannes Gutenberg University, Mainz, Germany, [7]State Key Laboratory for Mineral Deposits Research, School of Earth Sciences & Engineering, Frontiers Science Center for Critical Earth Material Cycling, Nanjing University, Nanjing, China

Abstract The Hangenberg Crisis coincided with a large decline of biodiversity and widespread anoxia in the end-Devonian ocean. Previous research attributed marine anoxia to the spread of deeply-rooted plants and/or increased volcanism on the continents, but crucial links have not been thoroughly explored. Herein, we propose enhanced weathering as a key trigger, as evidenced by a negative shift (~8‰) in lithium isotopes and a coupled response in carbon isotopes of marine carbonates in South China. Our findings imply that rapid weathering of crustal rocks increased nutrient delivery to the ocean, as indicated by an increase in the carbonate-associated phosphate levels, contributing to oceanic eutrophication. In the absence of massive volcanic emissions and intense orogeny, the cause of enhanced continental weathering was likely the expansion of the terrestrial rhizosphere, highlighting the potential for land plant evolution to initiate weathering changes of sufficient severity to trigger a major bio/environmental crisis in the Earth system.

Plain Language Summary The colonization of land plants during the Devonian is believed to have played a key role in regulating Earth's climate. The initially rapid expansion of seed plants into unvegetated or sparsely vegetated uplands is considered to have caused enhanced rock dissolution relative to clay formation on end-Devonian continents. As a consequence, larger amounts of isotopically-light lithium were transported to the ocean via rivers, resulting in a distinct negative excursion in seawater lithium isotopes. Concurrently, increased riverine nutrient delivery stimulated marine primary production and thus facilitated the expansion of oceanic anoxia. As a result, drawdown of atmospheric CO_2 resulted in climatic cooling, which together with widespread seafloor anoxia, triggered the major biotic turnover known as the "Hangenberg Crisis".

Key Points:

- Negative shift in carbonate lithium isotopes records major enhancement of continental weathering during the end-Devonian
- Enhanced chemical weathering increased riverine nutrient delivery and contributed to widespread marine anoxia and the Hangenberg Crisis
- Rapid expansion of seed plants in sparsely vegetated uplands may account for weathering-driven climatic cooling and oceanic changes

Supporting Information:

Supporting Information may be found in the online version of this article.

Correspondence to:

W. Qie and J. Zhang,
wkqie@nigpas.ac.cn;
jpzhang@nigpas.ac.cn

Citation:

Qie, W., Zhang, J., Luo, G., Algeo, T. J., Chen, B., Xiang, L., et al. (2023). Enhanced continental weathering as a trigger for the end-Devonian Hangenberg Crisis. *Geophysical Research Letters*, *50*, e2022GL102640. https://doi.org/10.1029/2022GL102640

Received 4 JAN 2023
Accepted 23 MAY 2023

Author Contributions:

Conceptualization: Wenkun Qie, Junpeng Zhang, Thomas J. Algeo, Xiangdong Wang
Data curation: Junpeng Zhang
Formal analysis: Genming Luo, Bo Chen, Lei Xiang, Xianyi Liu, Philip A. E. Pogge von Strandmann
Funding acquisition: Wenkun Qie

1. Introduction

The end-Devonian (~359 Ma) Hangenberg Crisis (HC) was a first-order Phanerozoic mass extinction associated with the final demise of stromatoporoid reefs in the ocean and a major turnover of higher-plant communities on land (Marshall et al., 2020; Yao et al., 2020). It coincided with widespread black shale, abrupt glacial-interglacial fluctuations, and major $\delta^{13}C$ variations within a time span of ~100–300 Kyr (Kaiser et al., 2016; Myrow et al., 2014). Multiple hypotheses have been proposed for its trigger, including climatic and eustatic changes, marine anoxia, volcanism, land plant evolution, and combinations of these events, but the ultimate cause(s) remain elusive (Kaiser et al., 2008, 2016; Rakociński et al., 2020; Zhang et al., 2020).

Enhanced continental weathering, triggered by the diversification and spread of vascular land plants, is believed to have strongly influenced Devonian global climate through drawdown of atmospheric CO_2 levels and modulation of Earth-surface biogeochemical cycles (Algeo et al., 2001; Le Hir et al., 2011). This hypothesis links marine anoxia and diversity loss to "continental greening," suggesting a strong terrestrial-marine teleconnection. Seawater strontium isotopes ($^{87}Sr/^{86}Sr$) exhibit a slow secular increase from ~0.7078 in the late Middle Devonian to a peak of ~0.7082 at the Devonian-Carboniferous (D-C) boundary (McArthur et al., 2020), and osmium isotopes ($^{187}Os/^{188}Os$) exhibit several sharp peaks over this ~25-Myr-long interval (Percival et al., 2019; Peucker-Ehrenbrink & Ravizza, 2020), suggesting sustained but episodic intensification of continental weathering.

Investigation: Wenkun Qie, Junpeng Zhang, Genming Luo, Thomas J. Algeo, Bo Chen, Kun Liang, Xianyi Liu, Philip A. E. Pogge von Strandmann, Jitao Chen
Methodology: Junpeng Zhang
Project Administration: Wenkun Qie
Supervision: Wenkun Qie, Xiangdong Wang
Validation: Wenkun Qie, Junpeng Zhang
Visualization: Wenkun Qie, Junpeng Zhang
Writing – original draft: Wenkun Qie, Junpeng Zhang
Writing – review & editing: Wenkun Qie, Junpeng Zhang, Genming Luo, Thomas J. Algeo, Bo Chen, Lei Xiang, Kun Liang, Xianyi Liu, Philip A. E. Pogge von Strandmann, Jitao Chen, Xiangdong Wang

However, interpretation of these isotopic systems as proxies for continental weathering is subject to ambiguity as their cycling also involves other processes and fluxes not directly linked to silicate weathering.

Marine carbonate lithium isotopes (δ^7Li_{carb}) have been utilized to identify weathering changes in both modern and ancient sedimentary systems (Misra & Froelich, 2012; Pogge von Strandmann et al., 2013, 2021) as they are sensitive mainly to silicate weathering, while seldom affected by carbonate weathering and not subject to fractionation by plants (Dellinger et al., 2015; Lemarchand et al., 2010). The oceanic Li cycle is primarily controlled by riverine and hydrothermal inputs, and the main sinks for aqueous Li are uptake by marine authigenic clays and low-temperature alteration of oceanic crust (Figure S1 in Supporting Information S1; Li & West, 2014). Therefore, δ^7Li_{carb} is better suited than either Sr or Os isotopes to probe global silicate weathering dynamics at intermediate timescales (i.e., hundreds of Kyr).

Here, we investigate weathering changes through the D-C transition based on a novel approach combining δ^7Li_{carb}, $\delta^{13}C_{carb}$, and $\delta^{13}C_{org}$, carbonate-associated phosphate (CAP), and trace elements, which were measured in a shallow-water carbonate succession in South China. In addition, we use mass balance models to generate quantitative constraints on weathering changes and the carbon cycle within the D-C boundary interval.

2. Geologic Setting

The 58-m-thick Longmenshan (LMS) section (GPS coordinates: 31°54′14″ N, 104°42′52″ E) is located in Mianyang City, Sichuan Province. It represents a shallow-water carbonate succession that accumulated on the northwestern margin of the South China Craton, close to the paleo-Equator and facing the Paleotethys Ocean to the south during the D-C transition (Figure 1). The section is stratigraphically complete, shows no evidence of sedimentary hiatuses, and brackets the HC event interval. The position of the HC horizon and D-C boundary are well-constrained by rugose coral biozones and key conodont elements (Figure 1). The Lower Hangenberg Crisis (LHC), which represents the main phase of the HC (i.e., equivalent to the lower and middle Hangenberg interval except for the "Drewer prelude" and the *ck*I Zone of Kaiser et al., 2016), consists of carbonate mudstone, dolostone and algal limestone devoid of metazoan macrofossils. The Upper Hangenberg Crisis (UHC), which represents a second crisis phase (i.e., equivalent to the *kockeli* Zone of Kaiser et al., 2016), consists of lime mudstone, bioclastic wackestone and argillaceous limestone containing non-dissepimented rugose corals, brachiopods and gastropods (Figure 1). Based on the Devonian timescale of Becker et al. (2012), the LHC is ~0.22 Myr and the UHC is ~0.19 Myr in duration. The LMS section accumulated at a high average sedimentation rate (>~23 m/Myr), thus providing enhanced stratigraphic resolution through the D-C transition interval.

3. Methods

A total of 243 predominantly bulk calcite samples was collected at LMS at an average spacing of ~25 cm (Figure 2). Samples were prepared and analyzed for δ^7Li_{carb}, $\delta^{13}C_{carb}$, and $\delta^{13}C_{org}$, major and trace elements at the State Key Laboratory of Palaeobiology and Stratigraphy, Nanjing Institute of Geology and Palaeontology, Chinese Academy of Sciences (NIGPAS). Ten replicate samples were analyzed in the LOGIC laboratories at University College London (UCL) to verify our δ^7Li_{carb} profile and to test for quality control. In addition, the CAP analysis was based on the molybdenum-blue method and conducted in the Sedimentary Geochemistry and Biogeochemistry Laboratory at China University of Geosciences (Wuhan). Please check the Supporting Information S1 for analytical protocols and those data sets (Tables S2–S4 in Supporting Information S1).

4. Results

An abrupt negative shift of δ^7Li_{carb} from ~+18‰ to ~+10‰ started ~8 m below the LHC (Figure 2). Seawater lithium isotope compositions (δ^7Li_{SW}) were calculated based on a constant fractionation factor (~5‰) between seawater and carbonate precipitates (Pogge von Strandmann et al., 2013). $\delta^{13}C_{carb}$ shifts gradually from +2‰ to ~0‰ within the LHC and then rapidly to ~+4‰ at the base of UHC (i.e., the end-Devonian carbon isotope excursion, or EDICE) before shifting back to ~+2‰ in the *bransoni-mehli* biointerval (Figure 2). The major positive shift of the EDICE can be traced in the Midcontinent of North America, Europe, and other sections in South China (Kaiser et al., 2016; Qie et al., 2021), representing one of the largest $\delta^{13}C_{carb}$ shifts of the Phanerozoic. The content of CAP normalized to carbonate content (i.e., CAP/(Ca + Mg)) shows a distinct rise from ~0.01 to ~0.2 in the LHC before declining to ~0.02 in the UHC (Figure 2).

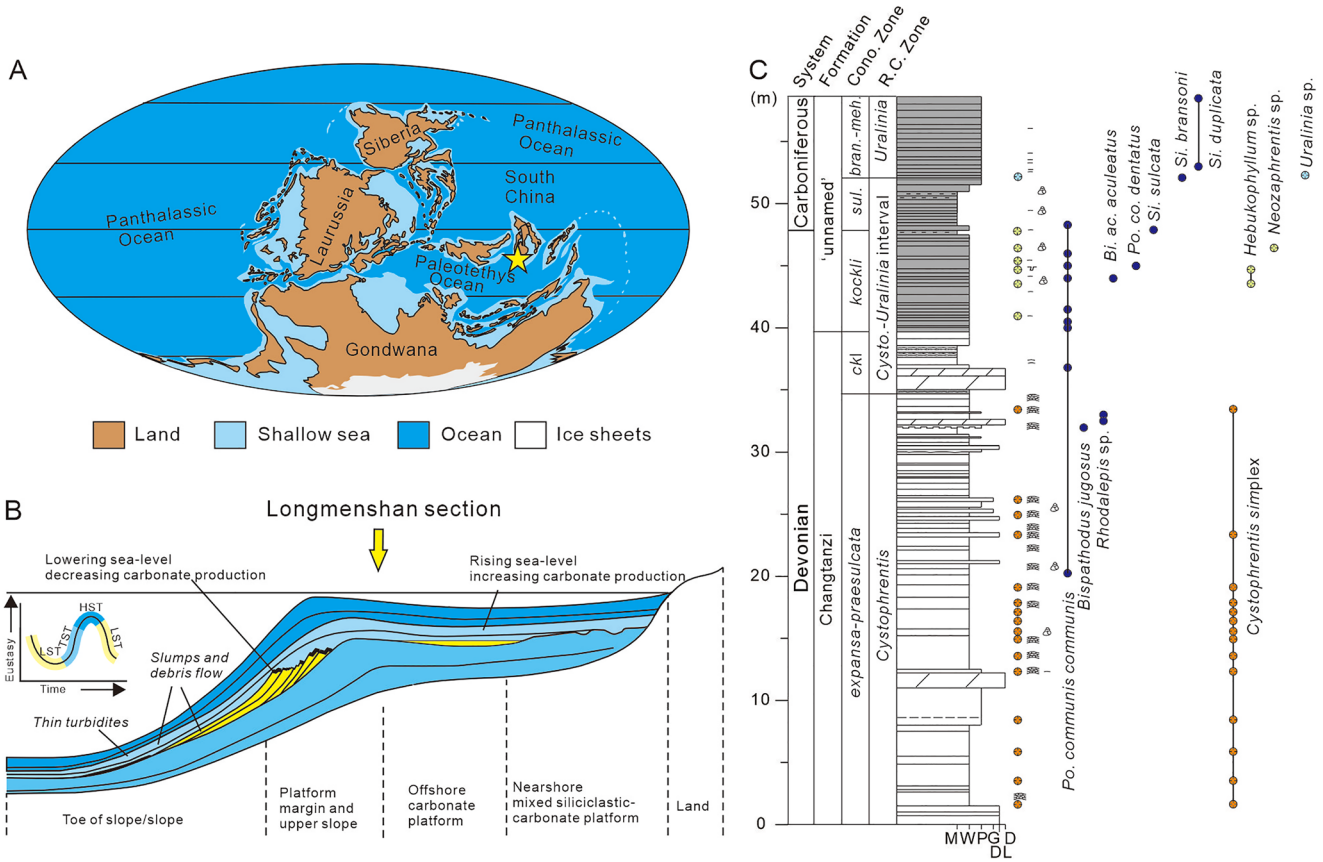

Figure 1. (a) Latest Devonian global paleogeographic reconstruction (base map courtesy of Ron Blakey, http://jan.ucc.nau.edu/~rcb7/) and the location of the studied LMS section (yellow star); (b) schematic cartoon to describe the depositional environment for the LMS section during the D-C transition; (c) Lithologic column, conodont and rugose coral zonations, and stratigraphic ranges of key conodonts and corals in the LMS section. Conodont biozonation after Becker et al. (2021) and rugose coral biozonation after Qie et al. (2021). The lithologic legend is shown in Figure 2, and the *bransoni-mehli* biointerval includes the *bransoni*, *duplicata* and *mehli* zones. Abbreviations: *bran.* = *bransoni*, *meh.* = *mehli*, *ck*I = *costatus-kockeli* interregnum, Cono. = Conodont, R.C. = Rugose coral, M = lime mudstone, W = wackestone, P = packstone, G = grainstone, DL = dolomitic limestone, D = dolostone.

If clay-associated Li was introduced during the leaching (chemical extraction) procedure or during diagenesis through cation exchange in clay minerals, then measured carbonate δ^7Li values would decrease and be accompanied by increases in Al/Ca (Pogge von Strandmann et al., 2013). The LMS section yields low values for Al/Ca (<0.8 mmol/mol) and Li/Ca (1–8 μmol/mol), and no correlation is observed between these ratios and δ^7Li_{carb} (Figures S2a and S2b in Supporting Information S1), indicating that silicate clays have not significantly influenced measured δ^7Li_{carb} values (Pogge von Strandmann et al., 2013). Study of modern systems indicates that meteoric and marine fluid-buffered diagenesis would induce significant (positive or negative) correlations between δ^7Li and Li/Ca, Sr/Ca and δ^{13}C, which can be used to evaluate whether measured δ^7Li_{carb} reflects changes in contemporaneous seawater composition (Dellinger et al., 2020; Wei et al., 2023). No observable correlations were identified among these proxies (Figures S2b–S2d in Supporting Information S1), suggesting no or minimal burial digenetic overprinting of the δ^7Li_{carb} profile of the LMS section. Additional determined carbonate Sr isotopes agree well with previous seawater $^{87}Sr/^{86}Sr$ profile (Table S5 in Supporting Information S1), which further support that the LMS carbonate may be a good archive of primary seawater signals. Moreover, low Mn/Ca ratios (<0.2 mol/mol) and Fe/Ca ratios (<1 mmol/mol) and their poor correlations with δ^7Li_{carb} suggest minimal influence of anoxic porewaters (Figures S2e and S2f in Supporting Information S1), the Li isotopic compositions of which are always higher than that of overlying seawater (Scholz et al., 2010). Low abundances of TOC (<0.5%) and U (mostly <1.5 ppm), along with the nature of the fossil assemblages, indicate deposition under uniformly oxic conditions. In addition, no obvious relationship between δ^7Li and stratigraphic variations in lithology is discernible (Figure 2). Therefore, we infer that the δ^7Li_{carb} shift reported for the LMS section represents a primary seawater signal.

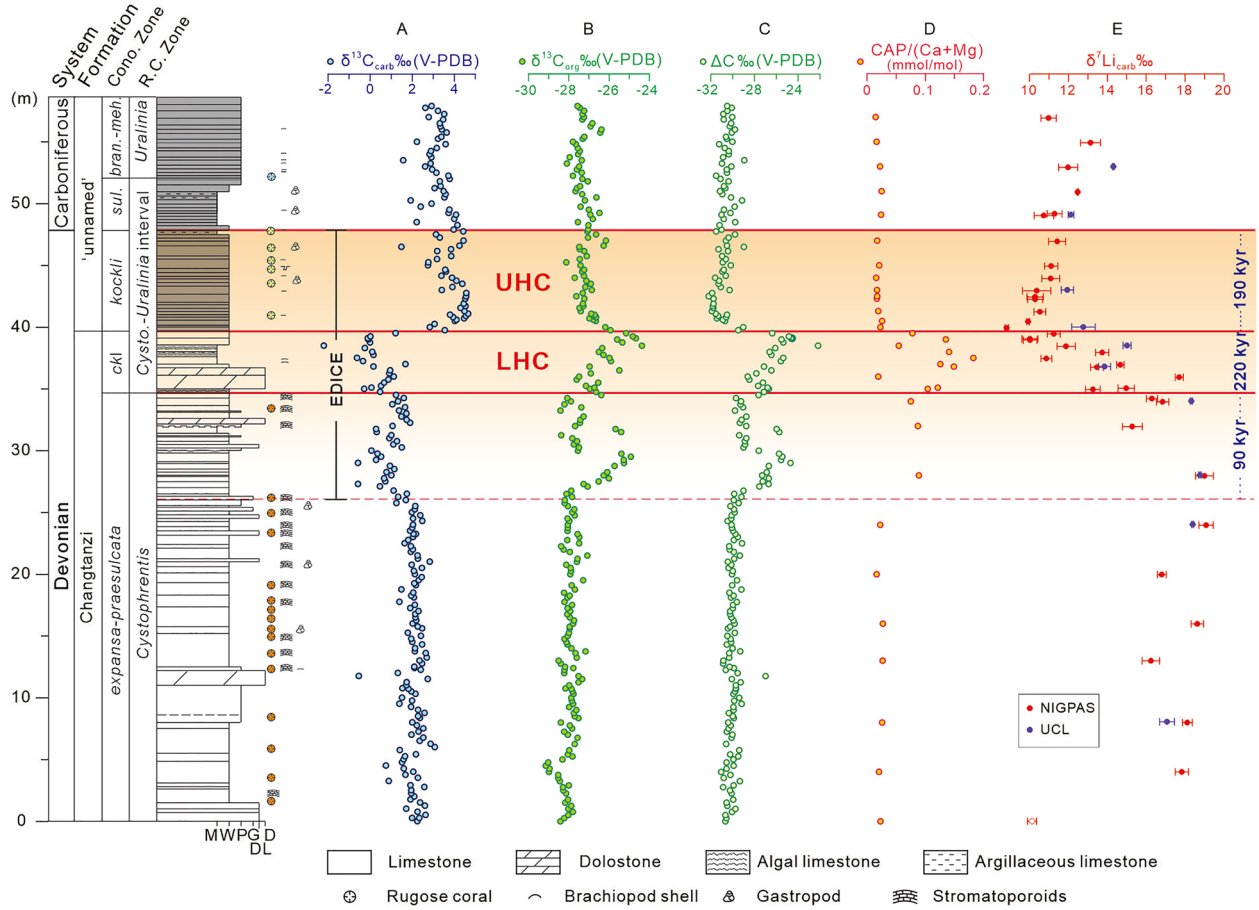

Figure 2. The LMS section with integrated geochemical profile including (a) $\delta^{13}C_{carb}$, (b) $\delta^{13}C_{org}$, (c) ΔC (=$\delta^{13}C_{org} - \delta^{13}C_{carb}$), (d) CAP/(Ca + Mg), and (e) $\delta^{7}Li_{carb}$ (red and purple solid circles represent duplicate analyses in NIGPAS and UCL, respectively, and the open red circle near the base is an isolated outlier). Conodont biozonation after Becker et al. (2021): *bran.* = *bransoni*, *meh.* = *mehli*, *ck*I = *costatus-kockeli* interregnum. R.C. = rugose coral.

Temperature-dependent fractionation of Li isotopes may occur during weathering and clay formation on continents such as δ^{7}Li variations during the Paleocene-Eocene Thermal Maximum (Pogge von Strandmann et al., 2021). As the temperature of deep-ocean is more constant, this effect during the removal of Li from the ocean is considered unable to induce observable seawater δ^{7}Li changes. In this study, the deviation is considered minor (<1.5‰ for −0.25‰/K) if compared with total ∼–8‰ shift in the δ^{7}Li of the marine carbonates (Pogge von Strandmann et al., 2021). Thus, this potential effect would not cause large uncertainty in our quantitative estimates of weathering changes through the EDICE.

5. Discussion

5.1. Li Isotope Variations and Weathering Process

We used a dynamic Li cycle model based on mass-balance equations (see modeling methods in Supporting Information S1) to investigate possible causes of the observed negative shift in $\delta^{7}Li_{SW}$ during the EDICE. As a starting point for modeling, we assumed that hydrothermal inputs (F_{hy}) can be constrained by mid-ocean ridge spreading rates, which were ∼1.43× present for the end-Devonian (Royer et al., 2014). In fact, uncertainty in the hydrothermal Li flux does not significantly affect our results, since a 200% increase in F_{hy} over a 300 Kyr interval causes only a small shift (∼–2.7‰) in $\delta^{7}Li_{SW}$ (Figure 3a).

Forcings associated with riverine Li inputs depend on both the source flux (F_{riv}) and its isotopic composition ($\delta^{7}Li_{riv}$). Further sensitivity tests were used to determine the potential effects of changes in these model parameters on $\delta^{7}Li_{SW}$ at a timescale of ∼300 Kyr (Figure 3a). First, if $\delta^{7}Li_{riv}$ is held constant at +10‰, an improbable

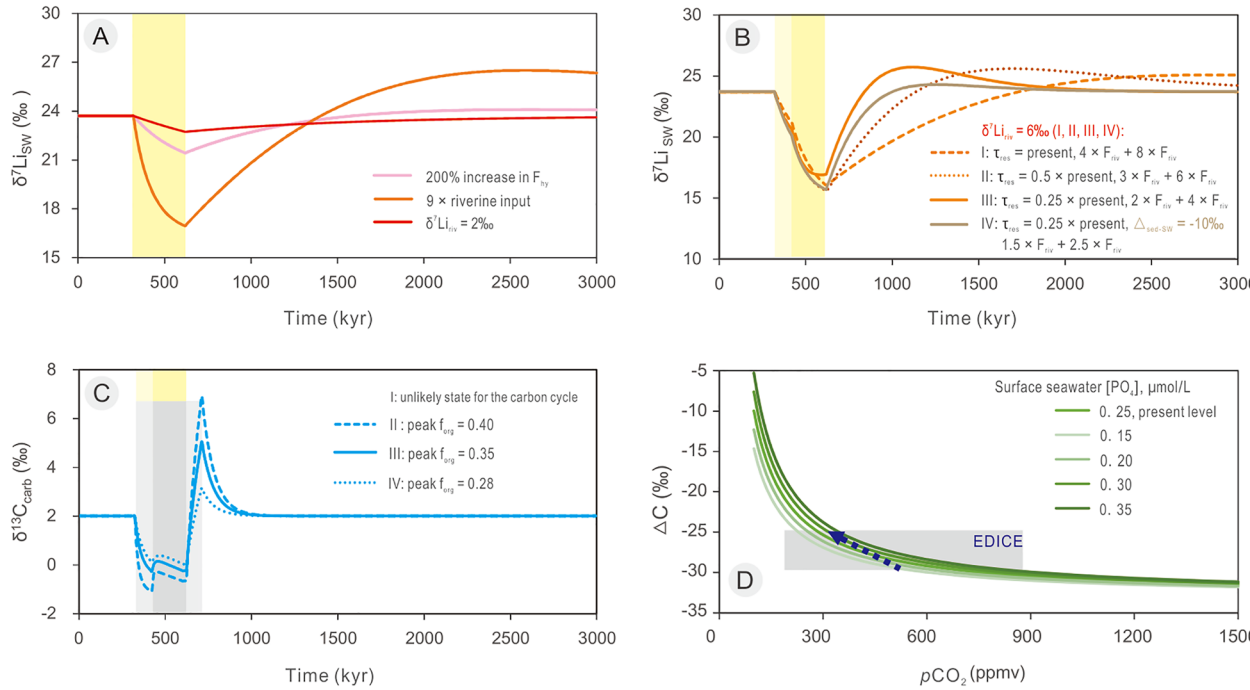

Figure 3. Model results for seawater δ^7Li and coupled carbonate $\delta^{13}C$: (a) the response of δ^7Li_{SW} to singular variation in hydrothermal input (increase by 200%), riverine Li input (×9), and relatively lower δ^7Li_{riv} (2‰) for 300 Kyr, respectively; (b) three assumed scenarios (I, II and III) with different residence time and variations in river Li flux and δ^7Li_{riv}; (c) the response of $\delta^{13}C_{carb}$ to increased weathering inputs and enhanced organic carbon burial. Yellow shades represent the interval of enhanced weathering, while gray shades denote the interval for increased burial of organic carbon.

increase (9×) in the F_{riv} is required to generate the observed −8‰ shift in δ^7Li_{SW}. Second, if the Li river flux is held constant, a reduction of δ^7Li_{riv} to +2‰ (n.b., equivalent to the upper crustal composition of 0‰ to +2‰; Figure S1 in Supporting Information S1) leads to only a minor negative shift (~–1.5‰) in δ^7Li_{SW} (Figure 3a). Thus, we infer that both an increase in riverine Li flux and a decrease in δ^7Li_{riv} were necessary to generate this negative δ^7Li_{SW} shift.

The δ^7Li_{carb} and CAP profiles for the LMS section suggest a two-step pattern in weathering changes, that is, an initial increase of river Li flux for ~100 Kyr followed by a larger pulse of ~200 Kyr (Figure 2). Larger and/or more rapid changes in δ^7Li_{SW} would have been possible if the Devonian seawater Li reservoir had a residence time shorter than in the modern ocean. Therefore, we investigated three scenarios with different residence times (present, 0.5× present, and 0.25× present) and assumed δ^7Li_{riv} of +6‰ (Table S1 in Supporting Information S1, Figure 3b). For the present residence time, a 4× increase in the riverine flux over 100 Kyr followed by an 8× increase over 200 Kyr are needed to produce the observed negative δ^7Li_{SW} shift (~–8‰) (Scenario I, Figure 3b). In comparison, the 0.5× and 0.25× residence times require riverine flux increases of ~3–6× and ~2–4× over 300 Kyr, respectively (Scenarios II and III, Figure 3b).

Low δ^7Li_{SW} values could potentially be achieved via enhanced reverse weathering with a smaller isotopic fractionation between seawater and authigenic clays (Scenario IV, Figure 3b), as recently inferred for the Permian-Triassic transition (Cao et al., 2022) and the early to middle Paleozoic (Kalderon-Asael et al., 2021). High reverse weathering rates would be achievable only in the event of high dissolved silica concentrations in the contemporaneous ocean. In the modern ocean, low rates of reverse weathering have been attributed to their silica-depleted condition, because of high biogenic opal mineralization (Isson & Planavsky, 2018). In the DCB interval, chert/siliceous rocks are widely present in deep-water basins (e.g., South China, Qie & Wang, 2012; Rhenish Region, Becker et al., 2021). In addition, radiolarians are abundant in the HC interval of the Moravian Karst, Czech Republic (Kumpan et al., 2014). The absence of a "chert gap" and global cooling preclude the possibility of high dissolved silica concentrations in Late Devonian seawater and thus imply little role for reverse weathering at that time.

During the LHC, increased riverine Li fluxes with low δ^7Li (+6‰) may indicate enhanced rock dissolution relative to clay formation on the continents, known as "weathering congruency" (Pogge von Strandmann et al., 2020).

However, δ^7Li_{riv} has an equivocal relationship to weathering intensity (i.e., the ratio of weathering rate relative to denudation rate, also "W/D"), given that low δ^7Li values are observed at both low and high weathering intensities, being linked to kinetically-limited and supply-limited weathering regimes, respectively (Dellinger et al., 2015). Our modeling results indicate that the major negative shift in δ^7Li_{SW} during the LHC could have resulted from a large increase in the riverine flux with a low δ^7Li_{riv} (Scenario III, Figure 3b), implying a kinetically-limited regime for the HC. However, greater weathering congruency, coupled to enhanced erosion due to higher runoff rates (which itself will drive W/D to lower values), is characteristic of warmer and wetter interglacials, rather than cooler intervals like the HC (Pogge von Strandmann et al., 2020; Zhang et al., 2022). Therefore, we infer that additional large-scale processes on the continents such as tectonic uplift and/or initial terrestrial afforestation may have altered weathering regimes during the interval of HC climatic cooling.

5.2. Response of Oceanic Carbon Cycle to Enhanced Weathering

The crust-like δ^7Li_{riv} and increased river Li flux during the HC suggests rapidly enhanced weathering of rocks and more efficient CO_2 drawdown, thus regulating the climate into cooling ages (Pogge von Strandmann et al., 2020). Meanwhile, enhanced silicate weathering would increase riverine nutrient inputs to the ocean, thus stimulating marine primary production and burial of organic carbon (Pogge von Strandmann et al., 2013). Therefore, the response of carbon cycle to enhanced weathering can be further explored by assuming the changes in weathering influx of the carbon cycle can be calibrated by the variations in riverine Li input as quantified above.

During the EDICE, the difference of $\delta^{13}C$ between inorganic carbon and organic matter (ΔC) fluctuated rapidly between $-30‰$ and $-25‰$, and may imply oscillations in atmospheric CO_2 levels and ocean phosphate concentrations, consistent with a rise in CAP at that time (Figures 2 and 3d). Scenario III shows that the EDICE can be reproduced via a stepwise increase (2–4×) in riverine Li input and consequent enhanced burial of organic carbon with f_{org} increasing from 0.23 to a peak of 0.35 over ~300 Kyr (Figure 3c). The interval of enhanced organic carbon burial is consistent with expansion of seafloor anoxia, as evidenced by carbonate $\delta^{238}U$ through the HC interval (Zhang et al., 2020). Therefore, the geochemical evidence and modeling results support that the establishment of extensive seafloor anoxia was fundamentally caused by enhanced continental weathering during the D-C transition.

5.3. Implications for the Hangenberg Crisis

In most Phanerozoic biocrises, continental silicate weathering usually served as a "climate thermostat" to regulate global climatic temperature, rather than as a cause of it. Both the end-Permian and end-Triassic mass extinctions were triggered by large igneous province (LIP) eruptions, accompanied by massive release of carbon to the Earth-surface system and ensuing hyperwarming events (e.g., Berner, 2002; Ruhl & Kürschner, 2011). Over the longer term, climatic warming promoted faster continental weathering and consumption of atmosphere CO_2, which slowly cooled the climate through a negative feedback.

In contrast, the HC was a "weathering-driven event," in which weathering rate changes were the cause, not the consequence, of contemporaneous climate change. Coeval shifts in δ^7Li_{carb}, CAP, and $\delta^{13}C$ indicate that enhanced continental weathering initiated increases in riverine nutrient fluxes and marine primary productivity, and further expansion of seafloor anoxia (Figure 2; Algeo et al., 2001; Zhang et al., 2020). The low, crust-like δ^7Li values and ΔC variations suggest brief but strong weathering congruency and efficient CO_2 drawdown during the LHC, thus triggering a ~100-200-Kyr-long phase of climatic cooling, as evidenced by the sudden appearance of Alpine-type glaciers in North and South America (Brezinski et al., 2010; Lakin et al., 2016). The ultimate result was widespread marine anoxia, carbonate factory shutdown, and, finally, the end-Devonian Hangenberg Crisis. A new, cooler steady-state climate mode emerged during the earliest Carboniferous, setting the stage for the Late Paleozoic Ice Age (Figure 4).

The ultimate cause of enhanced silicate weathering during the HC is still unknown. Late Devonian weathering rate changes have been attributed to increased global orogenic uplift (Averbuch et al., 2005) by analogy with the Late Cenozoic (Raymo & Ruddiman, 1992), or to LIP emplacement, but evidence for such activity during the Late Devonian is scant (Ernst & Youbi, 2017). Moreover, a peak in the seawater $^{87}Sr/^{86}Sr$ record near the D-C transition (Figure 4) precludes the possibility of intensified weathering of basaltic rocks (which are typically generated by LIPs). The most likely driver of a major increase in weathering intensity during the HC is a change

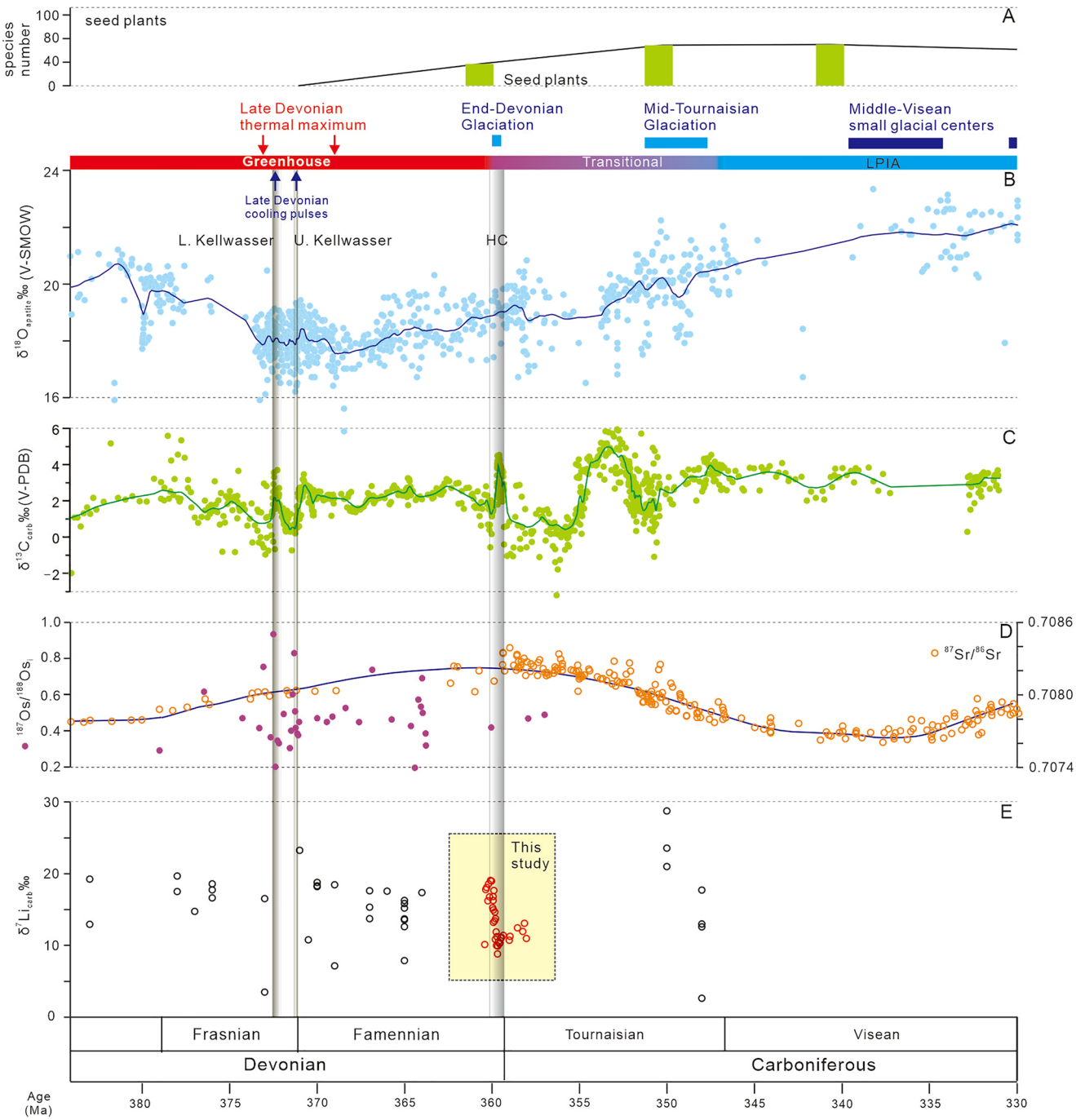

Figure 4. Integrative framework for Late Devonian to early Carboniferous including (a) species richness of global seed plants (after Chen, Chen, et al., 2021), (b) conodont $\delta^{18}O_{apatite}$ compiled from Chen, Ma, et al. (2021) and Grossman and Joachimski (2022), (c) bulk limestone $\delta^{13}C_{carb}$ from South China (Qie et al., 2021), (d) global $^{87}Sr/^{86}Sr$ profiles (after McArthur et al., 2020; Chen, Chen, et al., 2021) and $^{187}Os/^{188}Os$ values (Percival et al., 2019; Peucker-Ehrenbrink & Ravizza, 2020), and (e) $\delta^{7}Li_{carb}$ records (Kalderon-Asael et al., 2021 and this study–red open circles).

in terrestrial floras (Algeo et al., 2001)—more specifically, the rapid spread of seed plants, which first appeared in the early Late Devonian and had expanded globally by the end of the Devonian (Prestianni & Gerrienne, 2010). Most previous research indicates that terrestrialization promotes clay formation in the long term, resulting in higher riverine $\delta^{7}Li$ (Kalderon-Asael et al., 2021). We infer that the initial spread of seed plants into unvegetated or sparsely vegetated upland areas and drier continental interiors likely accelerated chemical dissolution of crustal rocks due to a combination of increased rhizosphere mass, more efficient mechanical breakup of

bedrock substrates (i.e., increasing the surface area for weathering), and an intensified hydrological cycle (Algeo & Scheckler, 2010; Pawlik et al., 2020; Xue et al., 2022). This process can explain the concurrent drawdown of atmospheric CO_2, elevated riverine nutrient fluxes, and expansion of marine anoxia that characterize the Hangenberg Crisis and that profoundly altered the Earth-surface system during the D-C transition.

Data Availability Statement

Supplements detailing methods and all data can be found in Supporting Information S1. All data are also stored in the Science Data Bank (https://www.scidb.cn/s/jMfm6j; DOI: https://doi.org/10.57760/sciencedb.08339). All samples collected as a part of this study are deposited at NIGPAS and can be checked via a direct link (http://bbg.nigpas.ac.cn/#/spDetail?sampleId=NIGPLMS1-243).

Acknowledgments
This work was supported by NFSC (42293280), Ministry of Science and Technology of the PRC (2019QZKK0706), Chinese Academy of Sciences (XDB26000000), China Scholarship Council (201804910207), and ERC Grant 682760 CONTROLPASTCO2.

References

Algeo, T. J., & Scheckler, S. E. (2010). Land plant evolution and weathering rate changes in the Devonian. *Journal of Earth Sciences*, *21*(S1), 75–78. https://doi.org/10.1007/s12583-010-0173-2

Algeo, T. J., Scheckler, S. E., & Maynard, J. B. (2001). Effects of the middle to late Devonian spread of vascular land plants on weathering regimes, marine biotas, and global climate. In P. Gensel & D. Edwards (Eds.), *Plants invade the land, evolutionary and environmental perspectives* (pp. 213–236). Columbia University Press.

Averbuch, O., Tribovillard, N., Devleeschouwer, X., Riquier, L., Mistiaen, B., & Van Vliet-Lanoe, B. (2005). Mountain building-enhanced continental weathering and organic carbon burial as major causes for climatic cooling at the Frasnian–Famennian boundary (c. 376 Ma)? *Terra Nova*, *17*(1), 25–34. https://doi.org/10.1111/j.1365-3121.2004.00580.x

Becker, R. T., Gradstein, F. M., & Hammer, O. (2012). The Devonian period. In F. M. Gradstein, J. G. Ogg, M. D. Schmitz, & G. M. Ogg (Eds.), *The geologic time scale 2012* (Vol. 2, pp. 559–601). Elsevier.

Becker, R. T., Hartenfels, S., & Kaiser, S. I. (2021). Review of Devonian-Carboniferous boundary sections in the Rhenish slate mountains (Germany). *Palaeobiodiversity and Palaeoenvironments*, *101*(2), 357–420. https://doi.org/10.1007/s12549-020-00469-6

Berner, R. A. (2002). Examination of hypotheses for the Permo–Triassic boundary extinction by carbon cycle modeling. *Proceedings of the National Academy of Sciences of the United States of America*, *99*(7), 4172–4177. https://doi.org/10.1073/pnas.032095199

Brezinski, D. K., Cecil, C. B., & Skema, V. W. (2010). Late Devonian glacigenic and associated facies from the central Appalachian Basin, eastern United States. *GSA Bulletin*, *122*(1–2), 265–281. https://doi.org/10.1130/b26556.1

Cao, C., Bataille, C. P., Song, H., Saltzman, M. R., Tierney Cramer, K., Wu, H., et al. (2022). Persistent late Permian to early Triassic warmth linked to enhanced reverse weathering. *Nature Geoscience*, *15*(10), 832–838. https://doi.org/10.1038/s41561-022-01009-x

Chen, B., Chen, J., Qie, W., Huang, P., He, T., Joachimski, M. M., et al. (2021). Was climatic cooling during the earliest Carboniferous driven by expansion of seed plants? *Earth and Planetary Science Letters*, *565*, 116953. https://doi.org/10.1016/j.epsl.2021.116953

Chen, B., Ma, X., Mills, B. J., Qie, W., Joachimski, M. M., Shen, S., et al. (2021). Devonian paleoclimate and its drivers: A reassessment based on a new conodont $\delta^{18}O$ record from South China. *Earth-Science Reviews*, *222*, 103814. https://doi.org/10.1016/j.earscirev.2021.103814

Dellinger, M., Gaillardet, J., Bouchez, J., Calmels, D., Louvat, P., Dosseto, A., et al. (2015). Riverine Li isotope fractionation in the Amazon River basin controlled by the weathering regimes. *Geochimica et Cosmochimica Acta*, *164*, 71–93. https://doi.org/10.1016/j.gca.2015.04.042

Dellinger, M., Hardisty, D. S., Planavsky, N. J., Gill, B. C., Kalderon-Asael, B., Asael, D., et al. (2020). The effects of diagenesis on lithium isotope ratios of shallow marine carbonates. *American Journal of Science*, *320*(2), 150–184. https://doi.org/10.2475/02.2020.03

Ernst, R. E., & Youbi, N. (2017). How Large Igneous Provinces affect global climate, sometimes cause mass extinctions, and represent natural markers in the geological record. *Palaeogeography, Palaeoclimatology, Palaeoecology*, *478*, 30–52. https://doi.org/10.1016/j.palaeo.2017.03.014

Grossman, E. L., & Joachimski, M. M. (2022). Ocean temperatures through the Phanerozoic reassessed. *Scientific Reports*, *12*(1), 8938. https://doi.org/10.1038/s41598-022-11493-1

Kaiser, S. I., Aretz, M., & Becker, R. T. (2016). *The global Hangenberg crisis (Devonian–Carboniferous transition): Review of a first-order mass extinction* (Vol. 423, pp. 387–437). Geological Society of London Special Publication.

Kaiser, S. I., Steuber, T., & Becker, R. T. (2008). Environmental change during the late Famennian and early Tournaisian (late Devonian-early Carboniferous): Implications from stable isotopes and conodont biofacies in southern Europe. *Geological Journal*, *43*(2–3), 241–260. https://doi.org/10.1002/gj.1111

Kalderon-Asael, B., Katchinoff, J. A., Planavsky, N. J., Hood, A. V. S., Dellinger, M., Bellefroid, E. J., et al. (2021). A lithium-isotope perspective on the evolution of carbon and silicon cycles. *Nature*, *595*(7867), 394–398. https://doi.org/10.1038/s41586-021-03612-1

Lakin, J. A., Marshall, J. E. A., Troth, I., & Harding, I. C. (2016). *Greenhouse to icehouse: A biostratigraphic review of latest Devonian-Mississippian glaciations and their global effects* (Vol. 423, pp. 439–464). Geological Society London Special Publications.

Le Hir, G., Donnadieu, Y., Goddéris, Y., Meyer-Berthaud, B., Ramstein, G., & Blakey, R. C. (2011). The climate change caused by the land plant invasion in the Devonian. *Earth and Planetary Science Letters*, *310*(3–4), 203–212. https://doi.org/10.1016/j.epsl.2011.08.042

Lemarchand, E., Chabaux, F., Vigier, N., Millot, R., & Pierret, M. C. (2010). Lithium isotope systematics in a forested granitic catchment (Strengbach, Vosges Mountains, France). *Geochimica et Cosmochimica Acta*, *74*(16), 4612–4628. https://doi.org/10.1016/j.gca.2010.04.057

Li, G., & West, A. J. (2014). Evolution of Cenozoic seawater lithium isotopes: Coupling of global denudation regime and shifting seawater sinks. *Earth and Planetary Science Letters*, *401*, 284–293. https://doi.org/10.1016/j.epsl.2014.06.011

Marshall, J. E., Lakin, J., Troth, I., & Wallace-Johnson, S. M. (2020). UV-B radiation was the Devonian-Carboniferous boundary terrestrial extinction kill mechanism. *Science Advances*, *6*(22), eaba0768. https://doi.org/10.1126/sciadv.aba0768

McArthur, J. M., Howarth, R. J., Shields, G. A., & Zhou, Y. (2020). Strontium isotope stratigraphy. In F. M. Gradstein, et al. (Eds.), *Geologic time scale 2020* (pp. 211–238). Elsevier.

Misra, S., & Froelich, P. N. (2012). Lithium isotope history of Cenozoic seawater: Changes in silicate weathering and reverse weathering. *Science*, *335*(6070), 818–823. https://doi.org/10.1126/science.1214697

Myrow, P. M., Ramezani, J., Hanson, A. E., Bowring, S. A., Racki, G., & Rakociński, M. (2014). High-precision U-Pb age and duration of the latest Devonian (Famennian) Hangenberg event, and its implications. *Terra Nova*, *26*(3), 222–229. https://doi.org/10.1111/ter.12090

Pawlik, Ł., Buma, B., Šamonil, P., Kvaček, J., Gałązka, A., Kohout, P., & Malik, I. (2020). Impact of trees and forests on the Devonian landscape and weathering processes with implications to the global Earth's system properties–A critical review. *Earth-Science Reviews*, *205*, 103200. https://doi.org/10.1016/j.earscirev.2020.103200

Percival, L. M. E., Selby, D., Bond, D. P. G., Rakociński, M., Racki, G., Marynowski, L., et al. (2019). Pulses of enhanced continental weathering associated with multiple Late Devonian climate perturbations: Evidence from osmium-isotope compositions. *Palaeogeography, Palaeoclimatology, Palaeoecology*, *524*, 240–249. https://doi.org/10.1016/j.palaeo.2019.03.036

Peucker-Ehrenbrink, B., & Ravizza, G. E. (2020). Osmium isotope stratigraphy. In F. M. Gradstein, et al. (Eds.), *Geologic time scale 2020* (pp. 239–257). Elsevier.

Pogge von Strandmann, P. A., Jenkyns, H. C., & Woodfine, R. G. (2013). Lithium isotope evidence for enhanced weathering during Oceanic Anoxic Event 2. *Nature Geoscience*, *6*(8), 668–672. https://doi.org/10.1038/ngeo1875

Pogge von Strandmann, P. A., Jones, M. T., West, A. J., Murphy, M. J., Stokke, E. W., Tarbuck, G., et al. (2021). Lithium isotope evidence for enhanced weathering and erosion during the Paleocene-Eocene Thermal Maximum. *Science Advances*, *7*(42), eabh4224. https://doi.org/10.1126/sciadv.abh4224

Pogge von Strandmann, P. A., Kasemann, S. A., & Wimpenny, J. B. (2020). Lithium and lithium isotopes in Earth's surface cycles. *Elements*, *16*(4), 253–258. https://doi.org/10.2138/gselements.16.4.253

Prestianni, C., & Gerrienne, P. (2010). Early seed plant radiation: An ecological hypothesis. In M. Vecoli, G. Clément, & B. Meyer-Berthaud (Eds.), *The terrestrialization process: Modelling complex interactions at the biosphere-geosphere interface* (Vol. 339, pp. 71–80). Geological Society of London Special Publication.

Qie, W., Sun, Y., Guo, W., Nie, T., Chen, B., Song, J., et al. (2021). Devonian-Carboniferous boundary in China. *Palaeobiodiversity and Palaeoenvironments*, *101*(2), 589–611. https://doi.org/10.1007/s12549-021-00494-z

Rakociński, M., Marynowski, L., Pisarzowska, A., Bełdowski, J., Siedlewicz, G., Zatoń, M., et al. (2020). Volcanic related methylmercury poisoning as the possible driver of the end-Devonian Mass Extinction. *Scientific Reports*, *10*(1), 7344. https://doi.org/10.1038/s41598-020-64104-2

Raymo, M. E., & Ruddiman, W. F. (1992). Tectonic forcing of late Cenozoic climate. *Nature*, *359*(6391), 117–122. https://doi.org/10.1038/359117a0

Royer, D. L., Donnadieu, Y., Park, J., Kowalczyk, J., & Godderis, Y. (2014). Error analysis of CO_2 and O_2 estimates from the long-term geochemical model GEOCARBSULF. *American Journal of Science*, *314*(9), 1259–1283. https://doi.org/10.2475/09.2014.01

Ruhl, M., & Kürschner, W. M. (2011). Multiple phases of carbon cycle disturbance from large igneous province formation at the Triassic-Jurassic transition. *Geology*, *39*(5), 431–434. https://doi.org/10.1130/g31680.1

Scholz, F., Hensen, C., De Lange, G. J., Haeckel, M., Liebetrau, V., Meixner, A., et al. (2010). Lithium isotope geochemistry of marine pore waters–insights from cold seep fluids. *Geochimica et Cosmochimica Acta*, *74*(12), 3459–3475. https://doi.org/10.1016/j.gca.2010.03.026

Wei, G. Y., Zhang, F., Yin, Y. S., Lin, Y. B., von Strandmann, P. A. P., Cao, M., et al. (2023). A 13 million-year record of Li isotope compositions in island carbonates: Constraints on bulk inorganic carbonate as a global seawater Li isotope archive. *Geochimica et Cosmochimica Acta*, *344*, 59–72. https://doi.org/10.1016/j.gca.2023.01.013

Xue, J., Wang, J., Huang, P., Liu, L., Huang, T., Zhang, L., et al. (2022). The colonization of drylands by early vascular plants: Evidence from Early Devonian fossil soils and in situ plant traces from South China. *Earth-Science Reviews*, *237*, 104290. https://doi.org/10.1016/j.earscirev.2022.104290

Yao, L., Aretz, M., Wignall, P. B., Chen, J., Vachard, D., Qi, Y., et al. (2020). The longest delay: Re-emergence of coral reef ecosystems after the late Devonian extinctions. *Earth-Science Reviews*, *203*, 103060. https://doi.org/10.1016/j.earscirev.2019.103060

Zhang, F., Dahl, T. W., Lenton, T. M., Luo, G., Shen, S. Z., Algeo, T. J., et al. (2020). Extensive marine anoxia associated with the late Devonian Hangenberg crisis. *Earth and Planetary Science Letters*, *533*, 115976. https://doi.org/10.1016/j.epsl.2019.115976

Zhang, F., Dellinger, M., Hilton, R. G., Yu, J., Allen, M. B., Densmore, A. L., et al. (2022). Hydrological control of river and seawater lithium isotopes. *Nature Communications*, *13*(1), 3359. https://doi.org/10.1038/s41467-022-31076-y

References From the Supporting Information

Dodd, M. S., Zhang, Z., Li, C., Algeo, T. J., Lyons, T. W., Hardisty, D. S., et al. (2021). Development of carbonate-associated phosphate (CAP) as a proxy for reconstructing ancient ocean phosphate levels. *Geochimica et Cosmochimica Acta*, *301*, 48–69. https://doi.org/10.1016/j.gca.2021.02.038

Kaiser, S. I., Aretz, M., & Becker, R. T. (2016). The global Hangenberg crisis (Devonian–Carboniferous transition): Review of a first-order mass extinction. In R. T. Becker, P. Königshof, & C. E. Brett (Eds.), *Devonian climate, sea level and evolutionary events* (Vol. 423, pp. 387–437). Geological Society of London Special Publication.

Kump, L. R., & Arthur, M. A. (1999). Interpreting carbon-isotope excursions: Carbonates and organic matter. *Chemical Geology*, *161*(1–3), 181–198. https://doi.org/10.1016/s0009-2541(99)00086-8

Li, W., Liu, X. M., & Godfrey, L. V. (2019). Optimisation of lithium chromatography for isotopic analysis in geological reference materials by MC-ICP-MS. *Geostandards and Geoanalytical Research*, *43*(2), 261–276. https://doi.org/10.1111/ggr.12254

Lv, Y., Liu, S. A., Wu, H., Hohl, S. V., Chen, S., & Li, S. (2018). Zn-Sr isotope records of the Ediacaran Doushantuo formation in South China: Diagenesis assessment and implications. *Geochimica et Cosmochimica Acta*, *239*, 330–345. https://doi.org/10.1016/j.gca.2018.08.003

Mills, B. J., Krause, A. J., Scotese, C. R., Hill, D. J., Shields, G. A., & Lenton, T. M. (2019). Modelling the long-term carbon cycle, atmospheric CO_2, and Earth surface temperature from late Neoproterozoic to present day. *Gondwana Research*, *67*, 172–186. https://doi.org/10.1016/j.gr.2018.12.001

Pogge von Strandmann, P. A., Elliott, T., Marschall, H. R., Coath, C., Lai, Y. J., Jeffcoate, A. B., & Ionov, D. A. (2011). Variations of Li and Mg isotope ratios in bulk chondrites and mantle xenoliths. *Geochimica et Cosmochimica Acta*, *75*(18), 5247–5268. https://doi.org/10.1016/j.gca.2011.06.026

Pogge von Strandmann, P. A., Fraser, W. T., Hammond, S. J., Tarbuck, G., Wood, I. G., Oelkers, E. H., & Murphy, M. J. (2019). Experimental determination of Li isotope behaviour during basalt weathering. *Chemical Geology*, *517*, 34–43. https://doi.org/10.1016/j.chemgeo.2019.04.020

Qie, W., Ma, X., Xu, H., Qiao, L., Liang, K., Guo, W., et al. (2019). Devonian integrative stratigraphy and timescale of China. *Science China Earth Sciences*, *62*(1), 112–134. https://doi.org/10.1007/s11430-017-9259-9

Qie, W., Qiao, L., Liang, K., Guo, W., Song, J. J., Liu, F., et al. (2020). *Devonian stratigraphy and index fossils of China: Hangzhou* (p. 540). Zhejiang University Press.

Wang, X., Hu, K., Qie, W., Sheng, Q., Chen, B., Lin, W., et al. (2019). Carboniferous integrative stratigraphy and time scale of China. *Science China Earth Sciences*, *62*(1), 135–153. https://doi.org/10.1007/s11430-017-9253-7

Weis, D., Kieffer, B., Maerschalk, C., Barling, J., De Jong, J., Williams, G. A., et al. (2006). High-precision isotopic characterization of USGS reference materials by TIMS and MC-ICP-MS. *Geochemistry, Geophysics, Geosystems*, *7*(8), 30. https://doi.org/10.1029/2006gc001283

Kumpan, T., Bábek, O., Kalvoda, J., Frýda, J., & Matys Grygar, T. (2014). A high-resolution, multiproxy stratigraphic analysis of the Devonian–Carboniferous boundary sections in the Moravian Karst (Czech Republic) and a correlation with the Carnic Alps (Austria). *Geological Magazine*, *151*(2), 201–215. https://doi.org/10.1017/s0016756812001057

Qie, W., & Wang, X. (2012). Carboniferous-early Permian deep-water succession in northern margin of the Dian-Qian-Gui Basin and its sedimentary evolution. *Geological Science*, *47*(4), 1074–1081.

Isson, T. T., & Planavsky, N. J. (2018). Reverse weathering as a long-term stabilizer of marine pH and planetary climate. *Nature*, *560*(7719), 471–475. https://doi.org/10.1038/s41586-018-0408-4

Pogge von Strandmann, P. A., Desrochers, A., Murphy, M., Finlay, A. J., Selby, D., & Lenton, T. M. (2017). Global climate stabilisation by chemical weathering during the Hirnantian glaciation. *Geochemical Perspectives Letters*, *3*, 230–236. https://doi.org/10.7185/geochemlet.1726